Phonon localization in mesoscopic free-standing films

1995 J. Phys.: Condens. Matter 7 5177

(http://iopscience.iop.org/0953-8984/7/27/006)

J. Phys.: Condens. Matter 7 (1995) 5177–5193. Printed in the UK

Phonon localization in mesoscopic free-standing films

M P Blencowe

The Blackett Laboratory, Imperial College, London SW7 2BZ, UK

Received 14 February 1995

Abstract. We examine the recent proposal of N Perrin concerning the possibility of observing phonon localization in mesoscopic free-standing insulating films with surface roughness. As our model structure, we consider a sapphire film with thickness $D = 100$ Å, width $W = 1$ μm and length $L = 10$ μm and surface roughness parameters $\Delta = 0.3D$ and $\xi = 500$ Å, where Δ is the rms deviation of the surface from flatness and ξ the transverse correlation length. We derive an effective phonon transport time $\tau_{\text{eff}}(\omega)$ for surface roughness scattering and then use this to determine the approximate frequency range over which the phonon localization length is less than the film length and also obtain a rough estimate of the thermal conductivity in the temperature range where the effect of localization is strongest.

1. Introduction

In a recent paper [1], Perrin argued that Anderson localization of phonons might occur at low temperatures in a free-standing electrically insulating film of mesoscopic dimensions. In particular, she considered free-standing crystalline silicon films of thickness 100–200 Å and transverse dimensions of a few micrometres. The reasons why such an unusually small structure is favourable for localization are as follows. Generally, the least difficult way to probe the phonon transport properties of a solid is to measure the thermal conductivity as a function of temperature. Now, a necessary condition for phonon localization is that the inelastic scattering rate be less than the elastic scattering rate and this requires that we measure the thermal conductivity at low temperatures—typically not more than a few kelvin. At 1 K, the thermal phonon wavelength for silicon is about 800 Å and therefore a free-standing film 100–200 Å thick will be effectively two dimensional for phonon transport. Recall that the tendency towards localization grows as the dimension is reduced and thus low-dimensional transport is desirable.

We have so far not said anything about the film defects which are responsible for the elastic scattering. The elastic scattering must be strong enough that the localization length of the thermal phonons will be less than the film length. The crucial observation of Perrin is that the scale of the roughness of real surfaces and the thermal phonon wavelength at temperatures around 1 K are of the same order of magnitude. Thus, at low temperatures, we expect the thermal phonons will be strongly scattered by the surface roughness.

Using existing electron beam lithography and chemical etching techniques, it should be just possible to fabricate a free-standing film from some electrically insulating material having the above-quoted dimensions [2, 3, 4].

In the present paper, we shall determine the thermal conductivity at low temperatures of a free-standing film with rough surfaces. It is hoped that our obtained results will be of use

0953-8984/95/275177+17$19.50

in interpreting the thermal conductivity data of any relevant future experiment. In particular, our results should help to confirm the presence (or absence) of phonon localization.

In the next section, we begin with a description of the model free-standing structure to be investigated. Starting with the Kubo–Greenwood formula for the thermal conductivity, we then derive the lowest-order, 'diffuson' approximation to the thermal conductivity. The more technical parts of the calculation are given in the appendix. The diffuson approximation is conveniently expressed in kinetic theory form in terms of an effective, frequency-dependent phonon transport time $\tau_{\rm eff}(\omega)$.

In section 3, we use $\tau_{\rm eff}(\omega)$ to determine the approximate frequency range over which the phonon localization length is less than the length of the free-standing film. We then give a rough estimate of the thermal conductivity in the temperature range for which the effect of localization is strongest and compare with the conductivity when there is no localization because of possible strong inelastic processes.

At a formal level, the phonon thermal conductivity calculations given in the following two sections are very similar to the electrical conductivity calculations for a disordered metal or semiconductor. In the details, however, there are some intriguing differences between the phonon and electron scattering behaviour and hence in their respective localization properties. We point out these differences.

In the conclusion, we discuss some problems which must be addressed in order to improve our understanding of phonon localization.

2. Determination of the effective phonon transport time

2.1. The model

As our model structure, we consider a free-standing, crystalline sapphire film with mean thickness $D = 100$ Å, width $W = 1$ μm and length $L = 10$ μm. The film coordinates $(r_1, r_2, r_3) = (r_\parallel, r_3)$ satisfy $-\frac{1}{2}W \leqslant r_1 \leqslant \frac{1}{2}W$, $-\frac{1}{2}L \leqslant r_2 \leqslant \frac{1}{2}L$ and $-\frac{1}{2}D + h_{\rm l}(r_\parallel) \leqslant r_3 \leqslant \frac{1}{2}D + h_{\rm u}(r_\parallel)$, where $h_{\rm u}$ and $h_{\rm l}$ are the deviations from flatness of the upper and lower surfaces of the film, respectively. The deviations are defined such that $\overline{h_{\rm u}} = \overline{h_{\rm l}} = 0$, where the overlines denote an average over an ensemble of surface roughness realizations. We assume the deviations obey Gaussian correlation relations:

$$\begin{aligned} &\overline{h_{\rm u}(r_\parallel)h_{\rm u}(r'_\parallel)} = \overline{h_{\rm l}(r_\parallel)h_{\rm l}(r'_\parallel)} = \Delta^2 \exp[-\xi^{-2}(r_\parallel - r'_\parallel)^2] \\ &\overline{h_u(r_\parallel)h_{\rm l}(r'_\parallel)} = 0 \end{aligned} \tag{1}$$

where the latter relation means that there is no correlation between the roughness of the upper and lower surfaces. The parameter Δ is the root mean square deviation of the surface from flatness, while ξ is the transverse correlation length. We assume the upper and lower surfaces have the same values for these parameters which we take to be $\Delta = 0.3D$ and $\xi = 500$ Å. The other numbers we require are the density and bulk transverse and longitudinal sound velocities of sapphire: $\rho = 3.99$ g cm^{-3}, $c_{\rm t} = 6 \times 10^5$ cm s^{-1} and $c_{\rm l} = 11 \times 10^5$ cm s^{-1}. We set Planck's constant $\hbar$ and Boltzmann's constant k to unity in the calculations, reintroducing them only in the final expressions.

We consider sapphire because it is elastically isotropic to a good approximation, thus greatly simplifying the analysis. Silicon would probably be the preferred material for experiment, however. We expect a silicon free-standing film with the same dimensions and roughness parameters will have qualitatively the same thermal conductivity behaviour as a function of temperature.

The measured correlation functions of actual surfaces are often well approximated by a Gaussian [5]. However, in some cases an exponential function provides a better fit [6]. There are also surfaces which are fractal-like [7]. The nature of the surface roughness will clearly depend on the surface material and the method of surface preparation. We have chosen the Gaussian correlation function because it is the simplest to treat analytically.

2.2. *The phonon modes*

At temperatures around 1 K, the thermal phonon wavelength is several hundred ångströms and thus we can use the continuum approximation. The continuum equations of motion for the ith component of the displacement field of the film at location $\boldsymbol{r}$ and time t are [8]

$$\rho \frac{\partial^2 u_i}{\partial t^2}(\boldsymbol{r}, t) = c_{ijkl}(\boldsymbol{r}) \frac{\partial^2 u_k}{\partial r_j \partial r_l}(\boldsymbol{r}, t) + \frac{\partial c_{ijkl}}{\partial r_j}(\boldsymbol{r}) \frac{\partial u_k}{\partial r_l}(\boldsymbol{r}, t) \tag{2}$$

where we have neglected anharmonic terms. We use the convention of summing over repeating indices with $i, j, k, \ldots = 1, 2, 3$. The position-dependent, elastic modulus tensor $c_{ijkl}(\boldsymbol{r})$ satisfies

$$c_{ijkl}(\boldsymbol{r}) = [\theta(-r_3 + h_u(\boldsymbol{r}_\parallel) + \tfrac{1}{2}D) - \theta(-r_3 + h_l(\boldsymbol{r}_\parallel) - \tfrac{1}{2}D)]c_{ijkl} \tag{3}$$

with

$$c_{ijkl} = \lambda \delta_{ij}\delta_{kl} + \mu(\delta_{ik}\delta_{jl} + \delta_{il}\delta_{jk}) \tag{4}$$

where $\theta(\cdot)$ denotes the Heaviside step function and λ and μ are the Lamé constants, related to the bulk transverse and longitudinal velocities by

$$\begin{aligned} \mu &= \rho c_t^2 \\ \lambda &= \rho(c_l^2 - 2c_t^2). \end{aligned} \tag{5}$$

Equation (4) follows from the approximation of isotropy in the elastic properties of sapphire.

The normal mode solutions to (2) having wavelengths of several hundred ångströms are slowly varying on the scale Δ. Following [8], we can therefore approximate $c_{ijkl}(\boldsymbol{r})$ as

$$\begin{aligned} c_{ijkl}(\boldsymbol{r}) \approx\ & [\theta(-r_3 + \tfrac{1}{2}D) - \theta(-r_3 - \tfrac{1}{2}D)]c_{ijkl} \\ & + [h_u(\boldsymbol{r}_\parallel)\delta(-r_3 + \tfrac{1}{2}D) - h_l(\boldsymbol{r}_\parallel)\delta(-r_3 - \tfrac{1}{2}D)]c_{ijkl} \end{aligned} \tag{6}$$

and substituting into (2), we obtain

$$\begin{aligned} \rho \frac{\partial^2 u_i}{\partial t^2} \approx\ & c_{ijkl} \frac{\partial^2 u_k}{\partial r_j \partial r_l} - c_{i3kl} \frac{\partial u_k}{\partial r_l}[\delta(-r_3 + \tfrac{1}{2}D) - \delta(-r_3 - \tfrac{1}{2}D)] \\ & + c_{ijkl} \frac{\partial u_k}{\partial r_l} \frac{\partial}{\partial r_j}[h_u(\boldsymbol{r}_\parallel)\delta(-r_3 + \tfrac{1}{2}D) - h_l(\boldsymbol{r}_\parallel)\delta(-r_3 - \tfrac{1}{2}D)] = 0. \end{aligned} \tag{7}$$

The second term on the right-hand side of the '$\approx$' sign in (7) provides the boundary conditions, while the third term contains the surface roughness. The boundary conditions ensure that the stresses acting on the flat surfaces $r_3 = \pm\frac{1}{2}D$ vanish. We have the very same boundary conditions at the rough surfaces in the more exact equation (2). (In fact, the surface roughness *only* enters in the boundary conditions.) For electrons in a free-standing metal film with rough surfaces, the boundary conditions are quite different: the wave function must vanish at the rough surfaces. As we shall see below, one consequence of these different boundary conditions is the qualitatively different energy dependences of the phonon and electron elastic scattering times [9].

The Kubo–Greenwood formula for the thermal conductivity which we give below involves the advanced and retarded displacement–displacement Green functions which satisfy an equation similar to (7) (see equation (16)). A fruitful way to approximate the ensemble-averaged Green functions is to neglect the third term on the right-hand side of (7) incorporating the surface roughness and first solve for the normal modes of the flat film. The normal modes are then used to construct the flat surface Green functions. Finally, a series approximation to the averaged rough surface Green functions can be obtained in terms of the flat Green functions and a 'roughness potential' (see equation (21)). Therefore, let us neglect the surface roughness term in (7) for now and investigate the flat-film normal modes.

The normal modes of a free-standing film are discussed in many textbooks (cf. [10]). The most common choice of basis involves the transverse (shear horizontal) modes and the symmetric and antisymmetric Lamb wave modes. These modes are grouped into subbands. For each of the three types, we shall consider only modes of the lowest-frequency subband in our calculation of the transport time and thermal conductivity. Corrections arising from the next-to-lowest-frequency subband are briefly discussed at the end of section 3. The modes are

(a) transverse

$$\begin{aligned} u^{\mathrm{T}}_{k\alpha}(r,t) &= V^{-1/2}\epsilon_{\alpha\beta}\frac{k_\beta}{k}\exp[\mathrm{i}(k\cdot r-\omega_{\mathrm{T}}(k)t)] \\ u^{\mathrm{T}}_{k3}(r,t) &= 0 \\ \omega_{\mathrm{T}}(k) &= c_{\mathrm{T}}k = c_{\mathrm{t}}k \end{aligned} \tag{8}$$

(b) longitudinal

$$\begin{aligned} u^{\mathrm{L}}_{k\alpha}(r,t) &= V^{-1/2}\frac{k_\alpha}{k}\exp[\mathrm{i}(k\cdot r-\omega_{\mathrm{L}}(k)t)] \\ u^{\mathrm{L}}_{k3}(r,t) &= 0 \\ \omega_{\mathrm{L}}(k) &= c_{\mathrm{L}}k = 2c_{\mathrm{t}}\sqrt{1-(c_{\mathrm{t}}/c_{\mathrm{l}})^2}k \end{aligned} \tag{9}$$

where Greek indices $\alpha,\beta,\ldots = 1,2$ label components in the r_1 and r_2 directions and the wavevector satisfies $k = (k_\parallel, 0) = (2\pi m/W, 2\pi n/L, 0)$, $n, m = 0, \pm1, \pm2, \ldots$. The antisymmetric tensor $\epsilon_{\alpha\beta}$ satisfies $\epsilon_{12} = -\epsilon_{21} = 1$ and $\epsilon_{11} = \epsilon_{22} = 0$. $V = LWD$ is the volume of the film and c_{T} and c_{L} are the velocities of the transverse and longitudinal modes of the film, respectively. To obtain (9), we have expanded the lowest subband symmetric Lamb wave modes in powers of kD and neglected terms of order kD and higher. The lowest-subband antisymmetric Lamb wave modes for small kD are called 'flexural' modes. We shall neglect the flexural modes in the calculations below. The contribution to the thermal conductivity from the flexural modes is briefly discussed at the end of section 3.

2.3. The Kubo–Greenwood formula for the thermal conductivity

In an experiment to measure the thermal conductivity, a given amount of power $\dot{Q}$ is supplied to the film at, say, the $r_3 = -\frac{1}{2}L$ end, with the $r_3 = +\frac{1}{2}L$ end kept at a fixed temperature T_1. The thermal conductivity of the film is then

$$\kappa = \frac{\dot{Q}/W}{(T_0 - T_1)/L} \tag{10}$$

where T_0 is the measured temperature at $r_3 = -\frac{1}{2}L$ and the power supplied is such that $(T_0 - T_1) \ll T_1$.

The Kubo–Greenwood formula provides a suitable starting point for an approximate evaluation of the thermal conductivity of the film which can be compared with experiment. The formula for the thermal conductivity is [11]

$$\kappa := \frac{1}{2}(\kappa_{11}+\kappa_{22}) = \frac{1}{2}\sum_{\alpha=1}^{2}\lim_{s\to 0}\left\{\frac{D}{TV}\int_0^\beta d\beta' \int_0^\infty dt\, e^{-st} \times Z^{-1}\,\mathrm{Tr}[\exp(-\beta\hat{H})\hat{J}_\alpha(-t-i\beta')\hat{J}_\alpha(0)]\right\} \tag{11}$$

where $\beta = T^{-1}$, $\hat{H}$ and $\hat{J}_\alpha(t)$ are the Hamiltonian and the energy current operators, respectively, and Z is the partition function. This formula holds under quite general assumptions concerning the lattice dynamics [11]. Using the elastic continuum equations of motion (2) to approximate the lattice dynamics and neglecting terms in the formula for $\hat{J}_\alpha(t)$ which are higher than quadratic order in the displacement field and momentum operators, we can express (11) in terms of the displacement–displacement Green functions. Following the derivations in [12] and [13], we obtain

$$\kappa = \frac{1}{2}\sum_{\alpha=1}^{2}\frac{D}{4\pi TV}\int_0^\infty d\omega\,\omega^2\frac{\partial}{\partial\omega}\left(\frac{1}{e^{\beta\omega}-1}\right)E_{\alpha imj}E_{\alpha knl} \times \int_V dr \int_V dr' \left(\frac{1}{2}\overline{\frac{\partial^2 G_{il}}{\partial r'_n \partial r_m}(r,r';\omega-i0)G_{kj}(r',r;\omega-i0)} + \frac{1}{2}\overline{\frac{\partial^2 G_{il}}{\partial r'_n \partial r_m}(r,r';\omega+i0)G_{kj}(r',r;\omega+i0)} - \overline{\frac{\partial^2 G_{il}}{\partial r'_n \partial r_m}(r,r';\omega+i0)G_{kj}(r',r;\omega-i0)}\right) \tag{12}$$

where

$$E_{ijkl} := (-4\mu+2\lambda)\delta_{ik}\delta_{jl} - 2\lambda(\delta_{il}\delta_{jk}+\delta_{ij}\delta_{kl}) \tag{13}$$

and where the retarded Green function is defined as

$$G_{ij}(r,r';\omega+i0) := \int_{-\infty}^{+\infty} d(t-t')\,\exp[i\omega(t-t')]\{-i\theta(t-t')\langle[\hat{u}_i(r,t),\hat{u}_j(r',t')]\rangle\} \tag{14}$$

and the advanced Green function is

$$G_{ij}(r,r';\omega-i0) := \int_{-\infty}^{+\infty} d(t-t')\,\exp[i\omega(t-t')]\{+i\theta(t'-t)\langle[\hat{u}_i(r,t),\hat{u}_j(r',t')]\rangle\} \tag{15}$$

with $\langle\cdots\rangle := Z^{-1}\,\mathrm{Tr}[\exp(-\beta\hat{H})\cdots]$. In (12), we have also averaged over an ensemble of surface roughness realizations, as indicated by the overlines.

Equation (12) is very similar in form to the expression for the electrical conductivity in terms of the advanced/retarded electron Green functions [14]. This close similarity enables us to use many of the approximation techniques developed for electrical conductivity calculations in order to evaluate the thermal conductivity. The first step is to apply these techniques to solve approximately for the averaged one-phonon Green functions $\overline{G_{ij}(r,r';\omega\pm i0)}$. The second step is to obtain an approximation to the averaged two-phonon Green functions $\overline{G_{ij}(r,r';\omega\pm i0)G_{kl}(r',r;\omega\pm i0)}$ in terms of the averaged one-phonon Green functions. We give these steps in the following two subsections.

2.4. The one-phonon Green functions

The integral form of the equations of motion for the one-phonon Green functions is (cf. equation (7)) [8, 15]

$$G_{ij}(r, r'; \omega \pm i0) = G^{(0)}_{ij}(r, r'; \omega \pm i0) - \int_V dr'' G^{(0)}_{ik}(r, r''; \omega \pm i0) L_{kl}(r'') G_{lj}(r'', r'; \omega \pm i0) \tag{16}$$

where

$$L_{ij}(r) := c_{ikjl}\left[\delta(-r_3 + \tfrac{1}{2}D)\left(\frac{\partial h_u}{\partial r^k}(r_\parallel) - \delta_{k3} h_u(r_\parallel)\frac{\partial}{\partial r^3}\right) - \delta(-r_3 - \tfrac{1}{2}D)\left(\frac{\partial h_l}{\partial r^k}(r_\parallel) - \delta_{k3} h_l(r_\parallel)\frac{\partial}{\partial r^3}\right)\right]\frac{\partial}{\partial r^l} \tag{17}$$

with c_{ijkl} given in (4). In terms of the normal modes (8) and (9), the flat surface Green functions are

$$G^{(0)}_{\alpha\beta}(r; \omega \pm i0) = \frac{1}{\rho V}\sum_k \left[\frac{1}{(\omega \pm i0)^2 - \omega_T^2(k)}\epsilon_{\alpha\rho}\epsilon_{\beta\sigma}\frac{k_\rho k_\sigma}{k^2} + \frac{1}{(\omega \pm i0)^2 - \omega_L^2(k)}\frac{k_\alpha k_\beta}{k^2}\right]\exp(ik \cdot r) \tag{18}$$

$$G^{(0)}_{3\alpha} = G^{(0)}_{\alpha 3} = G^{(0)}_{33} = 0$$

where k takes values as indicated immediately below equation (9). Formula (18) omits the flexural modes, as well as the sum over higher-frequency subband modes.

It is more convenient to work with the Fourier transforms of the Green functions. Equations (16) and (17) then become

$$G_{\mu\nu}(k, l; \omega \pm i0) = G^{(0)}_{\mu\nu}(k; \omega \pm i0)\delta_{k,l} + LW G^{(0)}_{\mu\rho}(k; \omega \pm i0)\sum_{k'} L_{\rho\sigma}(k, k') G_{\sigma\nu}(k', l; \omega \pm i0) \tag{19}$$

and

$$L_{\rho\sigma}(k, k') = [\lambda(k_\rho - k'_\rho)k'_\sigma + \mu(k_\nu - k'_\nu)k'_\nu\delta_{\sigma\rho} + \mu(k_\sigma - k'_\sigma)k'_\rho] \times [h_u(k - k') - h_l(k - k')] \tag{20}$$

where we have used the fact that $G^{(0)}$ (as given in (18)) and hence G do not depend on the r^3 coordinate.

Averaging the left- and right-hand sides of (19) over an ensemble of surface roughness realizations using for example the method given in [15], we obtain an equation for $\overline{G}$. To quadratic order in the surface roughness deviations h_u and h_l, we have

$$\overline{G}_{\mu\nu}(k; \omega \pm i0) = G^{(0)}_{\mu\nu}(k; \omega \pm i0) + G^{(0)}_{\mu\alpha}(k; \omega \pm i0) V_{\alpha\beta}(k; \omega \pm i0)\overline{G}_{\beta\nu}(k; \omega \pm i0) \tag{21}$$

where

$$V_{\alpha\beta}(k; \omega \pm i0) := LW\sum_s \mathcal{T}_{\alpha\nu}(k, s) G^{(0)}_{\nu\mu}(s; \omega \pm i0)\mathcal{T}_{\mu\beta}(s, k) \times \left\{2\pi(\Delta\xi)^2 \exp\left[-\frac{1}{4}\xi^2(k - s)^2\right]\right\} \tag{22}$$

and

$$\mathcal{T}_{\rho\sigma}(k, s) := \lambda(k_\rho - s_\rho)s_\sigma + \mu(k_\nu - s_\nu)s_\nu\delta_{\rho\sigma} + \mu(k_\sigma - s_\sigma)s_\rho. \tag{23}$$

In (22), the exponential term in curly brackets is just the Fourier transform of the surface roughness correlation function (1). The factor of two arises because both the upper and lower surfaces are rough and uncorrelated with each other, but characterized by the same statistical parameters. If the upper and lower surfaces were in fact identical (i.e. $h_u = h_l$) and hence correlated with each other, then we would have a factor of four instead.

Evaluating the sum over momentum s in (22) to obtain $V_{\alpha\beta}$ and then substituting the result in (21) and solving for $\overline{G}_{\mu\nu}$, we obtain

$$\overline{G}_{\alpha\beta}(k;\omega \pm i0) = (LW)^{-1}[\rho D(\omega^2 - \omega_T^2(k)) \pm i\Gamma_T(k;\omega)]^{-1}\epsilon_{\alpha\rho}\epsilon_{\beta\sigma}\frac{k_\rho k_\sigma}{k^2}$$
$$+(LW)^{-1}[\rho D(\omega^2 - \omega_L^2(k)) \pm i\Gamma_L(k;\omega)]^{-1}\frac{k_\alpha k_\beta}{k^2} \tag{24}$$

where

$$\Gamma_T(k;\omega) = B_T(k;\omega) + C_T(k;\omega) + E_L(k;\omega) \tag{25}$$

and

$$\Gamma_L(k;\omega) = D_L(k;\omega) + E_L(k;\omega) + A_T(k;\omega) + C_T(k;\omega) \tag{26}$$

with the functions A_T, B_T, C_T, D_L and E_L defined as follows:

$$A_T(k;\omega) := \frac{\pi\omega k^2\mu^2\Delta^2\xi^2}{4\rho D c_T^3}\exp\left[-\frac{\xi^2}{4}\left(\frac{\omega^2}{c_T^2}+k^2\right)\right]\left[\frac{\omega}{4c_T}\left(\frac{2\lambda}{\mu}+3\right)I_0\left(\frac{k\omega\xi^2}{2c_T}\right)\right.$$
$$-\frac{1}{4k}\left(k^2+\frac{\omega^2}{c_T^2}\right)I_1\left(\frac{k\omega\xi^2}{2c_T}\right) - \frac{\omega}{2c_T}\left(1+\frac{\lambda}{\mu}\right)I_2\left(\frac{k\omega\xi^2}{2c_T}\right)$$
$$\left.+\frac{1}{4k}\left(k^2+\frac{\omega^2}{c_T^2}\right)I_3\left(\frac{k\omega\xi^2}{2c_T}\right) - \frac{\omega}{4c_T}I_4\left(\frac{k\omega\xi^2}{2c_T}\right)\right] \tag{27}$$

$$B_T(k;\omega) := \frac{\pi\omega k^2\mu^2\Delta^2\xi^2}{4\rho D c_T^3}\exp\left[-\frac{\xi^2}{4}\left(\frac{\omega^2}{c_T^2}+k^2\right)\right]\left[\frac{\omega}{4c_T}I_0\left(\frac{k\omega\xi^2}{2c_T}\right)\right.$$
$$-\frac{1}{4k}\left(k^2+\frac{\omega^2}{c_T^2}\right)I_1\left(\frac{k\omega\xi^2}{2c_T}\right) + \frac{\omega}{c_T}I_2\left(\frac{k\omega\xi^2}{2c_T}\right)$$
$$\left.-\frac{3}{4k}\left(k^2+\frac{\omega^2}{c_T^2}\right)I_3\left(\frac{k\omega\xi^2}{2c_T}\right) + \frac{3\omega}{4c_T}I_4\left(\frac{k\omega\xi^2}{2c_T}\right)\right] \tag{28}$$

$$C_T(k;\omega) := \frac{\pi\omega k^2\mu^2\Delta^2\xi^2}{4\rho D c_T^3}\exp\left[-\frac{\xi^2}{4}\left(\frac{\omega^2}{c_T^2}+k^2\right)\right]\left[\frac{3\omega}{4c_T}I_0\left(\frac{k\omega\xi^2}{2c_T}\right)\right.$$
$$-\frac{1}{4k}\left(k^2+\frac{\omega^2}{c_T^2}\right)I_1\left(\frac{k\omega\xi^2}{2c_T}\right) - \frac{\omega}{2c_T}I_2\left(\frac{k\omega\xi^2}{2c_T}\right)$$
$$\left.+\frac{1}{4k}\left(k^2+\frac{\omega^2}{c_T^2}\right)I_3\left(\frac{k\omega\xi^2}{2c_T}\right) - \frac{\omega}{4c_T}I_4\left(\frac{k\omega\xi^2}{2c_T}\right)\right] \tag{29}$$

$$D_L(k;\omega) := \frac{\pi\omega k^2\mu^2\Delta^2\xi^2}{4\rho D c_L^3}\exp\left[-\frac{\xi^2}{4}\left(\frac{\omega^2}{c_L^2}+k^2\right)\right]$$
$$\times\left\{\frac{\omega}{2c_L}\left(\frac{\lambda}{\mu}+1\right)\left(\frac{3\lambda}{\mu}+4\right)I_0\left(\frac{k\omega\xi^2}{2c_L}\right)\right.$$
$$\left.-\left[\frac{1}{k}\left(\frac{\lambda}{\mu}+2\right)\left(\frac{\lambda}{\mu}+1\right)\left(\frac{\omega^2}{c_L^2}+k^2\right)+\frac{k}{2}\left(1+\frac{\lambda}{\mu}\right)\right]I_1\left(\frac{k\omega\xi^2}{2c_L}\right)\right.$$

$$+\left[\frac{\omega}{c_L}\left(\frac{3\lambda}{\mu}+4\right)+\frac{1}{2}\left(\frac{\lambda}{\mu}+1\right)\left(\frac{\lambda}{\mu}+2\right)\right]I_2\left(\frac{k\omega\xi^2}{2c_L}\right)$$
$$-\left[\frac{k}{2}\left(\frac{\lambda}{\mu}+3\right)+\frac{\omega^2}{kc_L^2}\left(\frac{\lambda}{\mu}+2\right)\right]I_3\left(\frac{k\omega\xi^2}{2c_L}\right)+\frac{\omega}{c_L}I_4\left(\frac{k\omega\xi^2}{2c_L}\right)\Bigg\} \tag{30}$$

$$E_L(k;\omega) := \frac{\pi\omega k^2\mu^2\Delta^2\xi^2}{4\rho D c_L^3}\exp\left[-\frac{\xi^2}{4}\left(\frac{\omega^2}{c_L^2}+k^2\right)\right]\Bigg\{\frac{\omega}{2c_L}\left(\frac{\lambda}{\mu}+3\right)I_0\left(\frac{k\omega\xi^2}{2c_L}\right)$$
$$-\left[\frac{k}{2}+\frac{\omega^2}{2c_L^2 k}\left(\frac{\lambda}{\mu}+2\right)\right]I_1\left(\frac{k\omega\xi^2}{2c_L}\right)$$
$$-\frac{\omega}{2c_L}\left(\frac{\lambda}{\mu}+2\right)I_2\left(\frac{k\omega\xi^2}{2c_L}\right)+\left[\frac{k}{2}+\frac{\omega^2}{2kc_L^2}\left(\frac{\lambda}{\mu}+2\right)\right]I_3\left(\frac{k\omega\xi^2}{2c_L}\right)$$
$$-\frac{\omega}{2c_L}I_4\left(\frac{k\omega\xi^2}{2c_L}\right)\Bigg\}. \tag{31}$$

The functions $I_n(x)$ are modified Bessel functions of integer order. In the calculation of $V_{\alpha\beta}$, we have neglected the real part. This gives a downward shift in the phonon velocities from their flat-surface values c_T and c_L.

In terms of the functions Γ_T and Γ_L, the transverse and longitudinal phonon elastic scattering times are

$$\tau_T(\omega) = \rho D\omega\Gamma_T^{-1}(k;\omega)\big|_{k=\omega/c_T} \tag{32}$$
$$\tau_L(\omega) = \rho D\omega\Gamma_L^{-1}(k;\omega)\big|_{k=\omega/c_L}. \tag{33}$$

For (ω/c_T), $(\omega/c_L) \ll \xi^{-1}$, we have the familiar 2D Rayleigh scattering frequency dependence $\tau_T(\omega)$, $\tau_L(\omega) \sim \omega^{-3}$. This strong frequency dependence should be contrasted with the approximately energy-independent behaviour of the electron elastic scattering time for $k < \xi^{-1}$ in a 2D metal film with rough surfaces [16]. As mentioned in subsection 2.2, these different dependences are a consequence of the fact that the lattice wave and electron wave satisfy different boundary conditions at the rough surface.

Another notable phonon scattering property not shared by electrons is the 'mixing' of the transverse and longitudinal polarizations. Note the E_L function in the definition of Γ_T (equation (25)) and the A_T and C_T functions in Γ_L (equation (26)). On scattering from the surface roughness, a transverse phonon can transform into a longitudinal phonon and vice versa, while for electrons the spin does not change. Note that this phonon transformation is not in contradiction with the assumption of elastic scattering. (This must be so since anharmonic terms do not appear in the equations of motion (2).) If a transverse phonon scatters into a longitudinal phonon, then the wavelength will increase by the amount $c_L/c_T > 1$ so that the frequency remains unchanged. Thus, Anderson localization can occur even though the scatterers change the polarization.

2.5. The two-phonon Green function and the effective transport time

In terms of the Fourier transforms of the Green functions, expression (12) for the thermal conductivity becomes

$$\kappa = \frac{DV}{8\pi T}E_{\alpha\beta\gamma\delta}E_{\alpha\rho\tau\sigma}\int_0^{+\infty}d\omega\,\omega^2\frac{\partial}{\partial\omega}\left(\frac{1}{e^{\beta\omega}-1}\right)\sum_{k,l}k_\gamma l_\tau$$
$$\times\Bigg[+\frac{1}{2}\overline{G_{\beta\sigma}(k,l;\omega+i0)G_{\delta\rho}(-k,-l;\omega+i0)}$$

$$+\frac{1}{2}\overline{G_{\beta\sigma}(\boldsymbol{k},l;\omega-\mathrm{i}0)G_{\delta\rho}(-\boldsymbol{k},-l;\omega-\mathrm{i}0)}$$

$$-\overline{G_{\beta\sigma}(\boldsymbol{k},l;\omega+\mathrm{i}0)G_{\delta\rho}(-\boldsymbol{k},-l;\omega-\mathrm{i}0)}\Big] \tag{34}$$

where we have used the identity

$$G_{\mu\nu}(\boldsymbol{k},l;\omega\pm\mathrm{i}0)=G_{\nu\mu}(-l,-\boldsymbol{k};\omega\pm\mathrm{i}0).$$

Following the Langer method [14] for determining the electrical conductivity, let us define

$$T^{+-}_{\alpha\beta\gamma\delta\rho}(\boldsymbol{k};\omega):=\sum_{l} l_\alpha\overline{G_{\beta\gamma}(\boldsymbol{k},l;\omega+\mathrm{i}0)G_{\delta\rho}(-\boldsymbol{k},-l;\omega-\mathrm{i}0)} \tag{35}$$

with analogous definitions for T^{++} and T^{--}. Using equations of motion (19) for the one-phonon Green functions, we obtain the following equation for T^{+-}:

$$T^{+-}_{\alpha\beta\gamma\delta\rho}(\boldsymbol{k};\omega)=k_\alpha\overline{G}_{\beta\gamma}(\boldsymbol{k};\omega+\mathrm{i}0)\overline{G}_{\delta\rho}(\boldsymbol{k};\omega-\mathrm{i}0)$$
$$+\overline{G}_{\beta\sigma}(\boldsymbol{k};\omega+\mathrm{i}0)\overline{G}_{\delta\tau}(\boldsymbol{k};\omega-\mathrm{i}0)\sum_{s}U_{\sigma\xi\tau\eta}(\boldsymbol{k},\boldsymbol{s};-\boldsymbol{k},-\boldsymbol{s};\omega)T^{+-}_{\alpha\xi\gamma\eta\rho}(\boldsymbol{s};\omega) \tag{36}$$

where U is the irreducible vertex. To lowest, quadratic order in the surface deviations h_u and h_l we have

$$U_{\sigma\xi\tau\eta}(\boldsymbol{k},\boldsymbol{s};-\boldsymbol{k},-\boldsymbol{s})\approx LW\mathcal{T}_{\sigma\xi}(\boldsymbol{k},\boldsymbol{s})\mathcal{T}_{\tau\eta}(-\boldsymbol{k},-\boldsymbol{s})\left\{2\pi(\Delta\xi)^2\exp\left[-\frac{\xi^2}{4}(\boldsymbol{k}-\boldsymbol{s})^2\right]\right\} \tag{37}$$

where $\mathcal{T}_{\alpha\beta}$ is defined in (23). The solution to (36) with U given by (37) is called the 'diffuson' approximation. Using similar methods to those of Langer [14], the diffuson approximations to T^{+-}, T^{++} and T^{--} are determined and then substituted into (34) and the sums over the various component indices and the wavevector k carried out. (The calculations are more involved than the analogous electron calculations because of the tensorial nature of the terms in (36).) Proceeding directly to the final result, we obtain

$$\kappa=-\frac{\hbar}{4\pi T}\int_0^\infty \mathrm{d}\omega\,\omega^3\frac{\partial}{\partial\omega}\left(\frac{1}{\mathrm{e}^{\beta\hbar\omega}-1}\right)2\tau_{\mathrm{eff}}(\omega) \tag{38}$$

where

$$\tau_{\mathrm{eff}}(\omega)=-\frac{D\omega}{4\rho}[\tilde{a}g-(\Gamma_{\mathrm{L}}-\tilde{g})(\Gamma_{\mathrm{T}}-a)]^{-1}[\tilde{c}f-(\Gamma_{\mathrm{L}}-\tilde{f})(\Gamma_{\mathrm{T}}-c)]^{-1}$$
$$\times\Big\{(\Gamma_{\mathrm{T}}-a)\Big[c_{\mathrm{L}}^{-4}(2\mu+\lambda)^2[\tilde{c}(f-\tfrac{4}{3}e)-(\Gamma_{\mathrm{T}}-c)(\Gamma_{\mathrm{L}}-(\tilde{f}-\tfrac{4}{3}\tilde{e}))]$$
$$-\tfrac{4}{3}c_{\mathrm{T}}^{-3}c_{\mathrm{L}}^{-1}(4\mu^2-\lambda^2)((\Gamma_{\mathrm{L}}-\tilde{f})e+f\tilde{e})\Big]$$
$$+\tilde{a}\Big[c_{\mathrm{L}}^{-3}c_{\mathrm{T}}^{-1}(4\mu^2-\lambda^2)[\tilde{c}(f-\tfrac{4}{3}e)-(\Gamma_{\mathrm{T}}-c)(\Gamma_{\mathrm{L}}-(\tilde{f}-\tfrac{4}{3}\tilde{e}))]$$
$$-\tfrac{4}{3}c_{\mathrm{T}}^{-4}(2\mu-\lambda)^2((\Gamma_{\mathrm{L}}-\tilde{f})e+f\tilde{e})\Big]$$
$$+(\Gamma_{\mathrm{L}}-\tilde{g})\Big[c_{\mathrm{T}}^{-4}(2\mu-\lambda)^2[f(\tilde{c}-\tfrac{4}{3}\tilde{b})-(\Gamma_{\mathrm{L}}-\tilde{f})(\Gamma_{\mathrm{T}}-(c-\tfrac{4}{3}b))]$$
$$-\tfrac{4}{3}c_{\mathrm{L}}^{-3}c_{\mathrm{T}}^{-1}(4\mu^2-\lambda^2)((\Gamma_{\mathrm{T}}-c)\tilde{b}+\tilde{c}b)\Big]$$
$$+g\Big[c_{\mathrm{T}}^{-3}c_{\mathrm{L}}^{-1}(4\mu^2-\lambda^2)[f(\tilde{c}-\tfrac{4}{3}\tilde{b})-(\Gamma_{\mathrm{L}}-\tilde{f})(\Gamma_{\mathrm{T}}-(c-\tfrac{4}{3}b))]$$
$$-\tfrac{4}{3}c_{\mathrm{L}}^{-4}(2\mu+\lambda)^2((\Gamma_{\mathrm{T}}-c)\tilde{b}+\tilde{c}b)\Big]\Big\}. \tag{39}$$

The functions $\Gamma_T(\omega)$ and $\Gamma_L(\omega)$ are defined as

$$\Gamma_T(\omega) := \Gamma_T(k;\omega)|_{k=\omega/c_T}$$
$$\Gamma_L(\omega) := \Gamma_L(k;\omega)|_{k=\omega/c_L}.$$

The functions $a(\omega)$, $b(\omega)$, ..., $\tilde{a}(\omega)$, $\tilde{b}(\omega)$, ... are given in the appendix.

Expression (38) for the thermal conductivity has been cast in the familiar kinetic theory form, with all the terms involving the phonon scattering conveniently grouped together in (39) as a single, effective phonon transport time $\tau_{\rm eff}(\omega)$. The factor two is required in (38) because there are two polarizations: longitudinal and transverse. Recall that the transport time is defined as the inverse of the difference between the 'scattering out' and 'scattering in' rates. If the scattering did not mix the transverse and longitudinal modes, then the diffuson approximation to the thermal conductivity would have the same form as (38) but with the term $2\tau_{\rm eff}$ replaced by the sum of the transverse and longitudinal phonon transport times. Because the surface roughness mixes the polarizations, the term $2\tau_{\rm eff}$ cannot be decomposed in this way and this is why we call $\tau_{\rm eff}$ an 'effective' transport time.

Expression (39) simplifies considerably at low and high frequencies. For the frequency range $\omega \ll c_L/\xi$, we have Rayleigh scattering:

$$\tau_{\rm eff}(\omega) \approx C c_L^2 D^2 \Delta^{-2} \xi^{-2} \omega^{-3} \tag{40}$$

where C is a dimensionless constant depending only on c_t and c_l, the bulk transverse and longitudinal velocities. For sapphire, $C \approx 0.11$.

For the frequency range $\omega \gg c_L/\xi$, we have

$$\tau_{\rm eff}(\omega) \approx \pi^{-\frac{1}{2}} \left[\frac{1}{15} \frac{(2+\lambda/\mu)^2}{(2-\lambda/\mu)^2} + \frac{1}{135} (c_L/c_T)^5 (2-\lambda/\mu)^2 \right] c_L^{-5} D^2 \Delta^{-2} \xi^5 \omega^4. \tag{41}$$

Note the strong ω^4 frequency dependence in (41). This is to be contrasted with the ω^2 dependence of the scattering times $\tau_L(\omega)$ and $\tau_T(\omega)$ for the same range $\omega \gg c_L/\xi$. Functions such as $\Gamma_T(\omega)$ and $a(\omega)$ in (39) coincide to leading non-vanishing order in an expansion in $c_T^2/(\omega\xi)^2$ and therefore their difference $\Gamma_T(\omega) - a(\omega)$ is smaller than $\Gamma_T(\omega)$ by the factor $c_T^2/(\omega\xi)^2$. This is the origin of the ω^2 difference in the frequency dependence.

The increase in the transverse and longitudinal scattering times and also transport time with increasing frequency $\omega \gg c_L/\xi$ can be understood by examining the form of the self-energy V defined in (22) and the irreducible vertex U defined in (37). For $k \gg \xi^{-1}$, the exponential term in V and U 'forces' the phonon to be forward scattered, i.e. $s \approx k$. However, the tensor term $\mathcal{T}_{\alpha\beta}(k, s)$ vanishes for $s = k$. Therefore, the strength of the interaction between the phonon and the surface roughness weakens as k increases, thus causing the phonon scattering times and transport time to increase.

From (40) and (41), we see that $\tau_{\rm eff}$ scales as $(D/\Delta)^2$ and, furthermore, $\tau_{\rm eff}(\omega)$ must have a minimum for some frequency ω close to c_L/ξ. Figure 1 shows $\tau_{\rm eff}$ versus frequency for the given parameters of our model structure. The effective transport time attains its *minimum value at* $\omega \approx 1.1 c_L/\xi$. *This result is the precise expression of Perrin's observation that phonons with wavelength of the same order of magnitude as the scale of the surface roughness are the most strongly scattered.* Note that a similar behaviour was observed by Seyler and Wybourne in their theoretical investigation of phonon scattering in narrow wires with surface roughness [17].

In our determination of the thermal conductivity, we neglected scattering from the film edges. Thus, we expect equation (39) will hold to good approximation only over the frequency range for which $\tau_{\rm eff}(\omega) c_L < W$, where W is the film width. (Recall that $c_L > c_T$ and therefore c_L sets the range.) For the parameters of our model structure, this condition

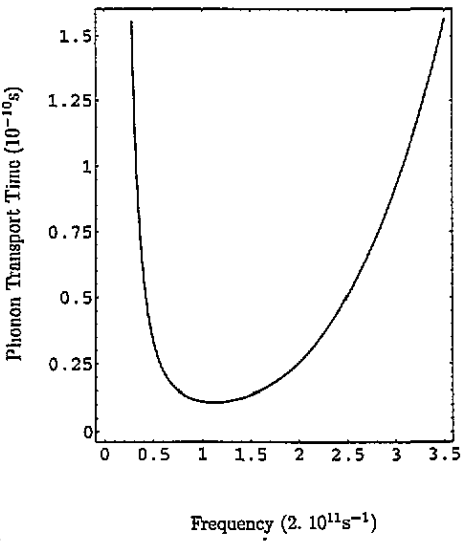

Figure 1. The effective phonon transport time versus frequency. The frequency is given in units of $c_L/\xi = 2 \times 10^{11}$ s^{-1}.

gives $0.33c_L/\xi < \omega < 3.1c_L/\xi$. We call this the strong-scattering frequency range. As we go to lower and higher frequencies, the transport time will deviate from (39) and tend towards a boundary scattering time, τ_b, which is expected to be approximately frequency independent and proportional to the film width:

$$\tau_b = \alpha W c_L^{-1} \tag{42}$$

where the parameter $\alpha > 1$ characterizes the specularity of the scattering from the side edges of the film. Neither is equation (42) expected to hold for arbitrarily low and high frequencies. For low enough frequencies, the scattering length will exceed the film length L, while for high enough frequencies, we expect the scattering length to be of the order of the film thickness D.

3. The thermal conductivity

In this section, we first determine the frequency range for which the phonon localization length $L_{loc}(\omega)$ is less than the length L ($= 10$ μm) of the free-standing film and then obtain estimates for the thermal conductivity versus temperature.

Most calculations of the phonon localization length treat phonons as scalars and assume the scatterers are pointlike and uncorrelated. As a consequence, the scattering potentials in the equations for the ensemble-averaged Green functions are isotropic. The localization length is relatively straightforward to estimate and is found to depend on the elastic scattering time. For the present problem, on the other hand, we see from equations (22), (23) and (37) that the scattering potential is highly anisotropic, even vanishing for forward scattering as was pointed out in subsection 2.5. Béal-Monod [18] has considered the more difficult problem of anisotropic scattering (for electrons) and has argued that the localization length estimates are identical in form to the estimates obtained assuming isotropic scattering, with the only difference that the scattering time is replaced by the transport time. We shall therefore assume a reasonable estimate for the phonon localization length is given by the

isotropic estimate with the elastic scattering length replaced by the effective transport time τ_{eff}.

We would like to determine the maximum and minimum frequencies for which $L_{\text{loc}}(\omega) < L$ and therefore require an estimate of $L_{\text{loc}}(\omega)$ for frequencies where $L_{\text{loc}}(\omega) > W$. Such an estimate can be obtained using the methods of Thouless [19,20]. The localization length estimate is [1]

$$L_{\text{loc}}(\omega) \approx \frac{1}{2\pi} W \omega \tau_{\text{eff}}(\omega) \tag{43}$$

giving a maximum frequency

$$\omega_{\max} \approx 3.1 \frac{c_{\text{L}}}{\xi} \tag{44}$$

for the condition $L_{\text{loc}}(\omega) < L$. On the other hand, there would appear not to be a minimum frequency: we have $L_{\text{loc}}(\omega) < L$ for $0.33 c_{\text{L}}/\xi < \omega < 3.1 c_{\text{L}}/\xi$, the strong-scattering range, and for $\omega < 0.33 c_{\text{L}}/\xi$ as well with τ_{eff} in (43) replaced by τ_{b} with specularity parameter α of order unity. However, as was pointed out in subsection 2.5, the boundary scattering estimate (42) does not hold for arbitrarily small ω. For large enough wavelength, we will have ballistic transport along the length of the film and therefore there must be a minimum frequency $\omega_{\min}$ for which $L_{\text{loc}}(\omega) < L$. We are unable to give an estimate for $\omega_{\min}$ using the present approximation methods, however, since they are appropriate only for the strong-scattering frequency range. A separate investigation would be required.

In order that a phonon be localized, it is necessary that the time taken for the phonon to diffuse along the localization length be less than the inelastic scattering time. Perrin [1] assumes the inelastic scatterers in the free-standing film can be modelled as two-level systems (TLS). For her estimates of the number density of TLSs and the coupling strength between the TLSs and the phonons, the localization length diffusion time is indeed less than the inelastic time when the localization length is less than the film length. However, it must be noted that there is a good deal of uncertainty concerning the nature of inelastic scatterers in disordered materials at low temperatures: very few experiments have been carried out on mesoscopic, free-standing films and therefore we cannot at present rule out the possibility of strong inelastic surface roughness and/or impurity scattering mechanisms.

Thus, in figure 2 we give two different possible estimates for the thermal conductivity versus temperature. The dashed curve assumes the phonons are *not* localized for $\omega < \omega_{\max}$, because of some strong inelastic scattering mechanism giving an inelastic scattering time which is smaller than the localization length diffusion time (but larger than τ_{eff}). This curve is a plot of (38), with $\tau_{\text{eff}}(\omega)$ replaced outside the strong-scattering frequency range by the boundary scattering time, τ_{b}, with specularity parameter $\alpha = 3$. This is clearly only a rough approximation: the actual transition from $\tau_{\text{eff}}(\omega)$ to τ_{b} will not be as abrupt.

The full curve is a rough estimate of the thermal conductivity assuming the phonons *are* localized for $\omega < \omega_{\max}$. The curve is simply a plot of (38) with τ_{eff} replaced by τ_{b} ($\alpha = 3$) and with lower frequency cut-off $\omega_{\max} = 3.1 c_{\text{L}}/\xi$ in the integration range.

If we could extend these two curves down to lower temperatures, then we would find they eventually coincided since, as discussed above, for sufficiently low frequencies the localization length will exceed the film length.

Given the magnitude of the difference between the two curves, it should be possible in an experiment which measures the thermal conductivity of a free-standing film with similar characteristics to those of our model structure to determine whether or not phonons are localized within the length of the film for the predicted frequency range.

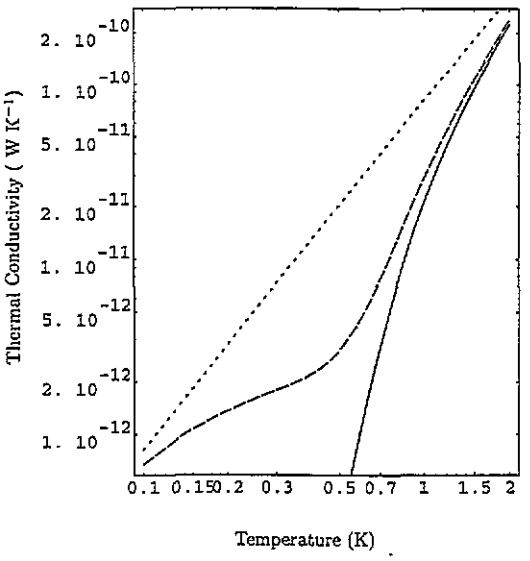

Figure 2. Estimates of the thermal conductivity versus temperature assuming phonons are either localized (full line) or not localized (dashed line). The reference curve (dotted line) assumes boundary scattering without localization.

The dotted reference curve in figure 2 assumes only boundary scattering ($\alpha = 3$) throughout the frequency range for 2D transport. Such a T^2-dependent curve is expected when there is no localization and also when the ratio Δ/D characterizing the degree of surface roughness is so small that $\tau_{\text{eff}}(\omega) > \tau_b$ for all ω. Comparing the other two curves with this reference curve, we see that a departure from T^2 behaviour in the measured thermal conductivity is a signal for the existence of a strong-scattering frequency range and/or phonon localization.

In our calculation of the thermal conductivity, only the lowest-frequency subband modes are taken into account (see subsection 2.2). The frequency at $k_\parallel = 0$ of the next-to-lowest transverse mode subband is $\pi c_T/D \approx 9.5 c_L/\xi$. The specific heat part of the thermal conductivity formula (38) is a maximum at this frequency when $T \approx 4.9$ K. The next-to-lowest-frequency subband modes are therefore expected to give only a small increase in the thermal conductivity estimates for the considered temperature range in figure 2.

The flexural modes were also neglected. For small kD, their flat-surface dispersion relation is $\omega(k) = 3^{-1/2} c_t (1 - c_t^2/c_l^2)^{1/2} Dk^2$. Therefore, their group velocity is of order kD less than the longitudinal and transverse velocities. At $T = 0.5$ K, $k_{\text{thermal}} D \approx D/\xi = 0.2$ and thus we expect the flexural modes to give a small contribution to the thermal conductivity for temperatures around 0.5 K and lower. Their contribution to the thermal conductivity at higher temperatures is not known. The contribution of the flexural modes to the thermal conductivity certainly requires further examination.

4. Conclusion

We have investigated phonon localization in a mesoscopic, free-standing sapphire film with rough surfaces. Perrin [1] argued that a mesoscopic free-standing structure is favourable for observing localization because of the strong elastic scattering due to the surface roughness

and the expected comparatively weak inelastic scattering due to two-level systems at low temperatures.

Most of the work involved calculating an effective phonon transport time (equations (39)–(41) and figure 1), which was then used to obtain an estimate of the frequency range for which the phonon localization length is less than the film length (equations (43) and (44)). Finally, rough estimates of the thermal conductivity versus temperature were plotted (figure 2) in the temperature range where effects due to localization are strongest.

While the methods used to calculate the phonon transport time and estimate the phonon localization length are very similar to the electron methods, there are significant differences between the behaviour of these quantities and their counterparts for electron transport in a free-standing metal film with rough surfaces. These differences are a consequence of the stress-free boundary conditions on the phonons at the film surface and also of the phonon having a polarization which can change when the phonon is scattered by the rough surface.

The calculations can be improved in several ways. The higher symmetric Lamb wave and transverse subband modes as well as the antisymmetric Lamb wave modes should be taken into account and the thermal conductivity calculation extended to lower and higher temperatures. Also, an actual surface will require a range of lengths for an accurate statistical description. The characterization of the surface roughness by a single correlation length is clearly an idealization. The consequences for the thermal conductivity of having a range of lengths should be investigated.

During the course of this investigation, two questions arose concerning phonon localization which are of a more general nature and not necessarily restricted to phonon transport in the free-standing structure considered here. Both questions have a bearing on the rôle phonon–phonon interactions play in phonon localization. Phonon–phonon interactions were neglected in the present work. It is expected that the most significant differences between phonon localization and localization in other wavelike systems arise when phonon–phonon interactions are taken into account. A recent investigation of the rôle of phonon–phonon interactions can be found in [21] (see also references therein). We now finish with an outline of these two questions.

(1) To what extent is it meaningful to treat the thermal phonons as (possibly) localized excitations as we have done in the present investigation? At non-zero temperatures, we expect phonon–phonon interactions to enable a phonon to 'hop' from one localized state to another, thus delocalizing the phonon and giving a non-zero thermal conductivity. In the case of electrons, the non-zero-temperature data for the electrical conductivity can be extrapolated to $T = 0$ in order to obtain the desired localization data. However, such an extrapolation cannot be carried out for the phonon thermal conductivity since at $T = 0$ there are obviously no thermal phonons.

(2) What rôle does the quantum nature of phonons play in localization? Planck's constant $\hbar$ does not appear in the estimate (43) for the localization length. The same formula would also apply for classical elastic wave transmission through a macroscopic, scaled-up version of the sapphire film (with suitably scaled-down wave frequency). Planck's constant only enters the specific heat part of the thermal conductivity formula (38). Differences between classical elastic wave localization and quantum phonon localization are expected to arise when anharmonic terms are included in the wave equation and the corresponding phonon–phonon interactions taken into account in the quantization of the wave equation.

Answers to these questions would help provide a better understanding of phonon localization as a phenomenon which is distinct from localization in other wave systems with disorder.

Acknowledgments

The author is grateful to A MacKinnon, E Hofstetter, P Šmilauer, A McLean and N Prokof'ev for helpful and stimulating discussions.

Appendix

We give here the explicit forms of the functions which appear in formula (39) for the effective transport time τ_{eff}. The functions $I_n(x)$ are modified Bessel functions of integer order. To shorten the equations, the arguments of the Bessel functions are given after each equation.

$$a := \frac{\pi\omega^4\mu^2\Delta^2\xi^2}{4\rho D c_{\mathrm{T}}^6}\exp\left(-\frac{\xi^2\omega^2}{2c_{\mathrm{T}}^2}\right)\left(-\frac{1}{2}I_0+\frac{1}{2}I_1-\frac{1}{2}I_2+I_3-\frac{1}{2}I_4+\frac{1}{4}I_5-\frac{1}{2}I_6+\frac{1}{4}I_7\right) \tag{A1}$$

where $I_n := I_n(\xi^2\omega^2/2c_{\mathrm{T}}^2)$,

$$b := \frac{\pi\omega^4\mu^2\Delta^2\xi^2}{4\rho D c_{\mathrm{T}}^6}\exp\left(-\frac{\xi^2\omega^2}{2c_{\mathrm{T}}^2}\right)\left(\frac{9}{16}I_1-\frac{3}{8}I_2-\frac{3}{8}I_3+\frac{3}{8}I_6-\frac{3}{16}I_7\right) \tag{A2}$$

where $I_n := I_n(\xi^2\omega^2/2c_{\mathrm{T}}^2)$,

$$c := \frac{\pi\omega^4\mu^2\Delta^2\xi^2}{4\rho D c_{\mathrm{T}}^6}\exp\left(-\frac{\xi^2\omega^2}{2c_{\mathrm{T}}^2}\right)\left(-\frac{1}{2}I_0+\frac{5}{4}I_1-I_2+\frac{1}{2}I_3-\frac{1}{2}I_4+\frac{1}{4}I_5\right) \tag{A3}$$

where $I_n := I_n(\xi^2\omega^2/2c_{\mathrm{T}}^2)$,

$$\begin{aligned} e := \frac{\pi\omega^4\mu^2\Delta^2\xi^2}{4\rho D c_{\mathrm{L}}^6}\exp\left[-\frac{\xi^2\omega^2}{4}(c_{\mathrm{T}}^{-2}+c_{\mathrm{L}}^{-2})\right]\Bigg[&-\frac{3c_{\mathrm{L}}}{4c_{\mathrm{T}}}\left(2+\frac{\lambda}{\mu}\right)I_0 \\ &+\left(\left(\frac{3c_{\mathrm{L}}}{4c_{\mathrm{T}}}\right)^2+\frac{3}{8}\left(2+\frac{\lambda}{\mu}\right)^2\right)I_1+\frac{3c_{\mathrm{L}}}{8c_{\mathrm{T}}}\left(2+\frac{\lambda}{\mu}\right)I_2 \\ &-\frac{9}{16}\left(\left(\frac{c_{\mathrm{L}}}{c_{\mathrm{T}}}\right)^2+\left(2+\frac{\lambda}{\mu}\right)^2\right)I_3+\frac{3c_{\mathrm{L}}}{4c_{\mathrm{T}}}\left(2+\frac{\lambda}{\mu}\right)I_4 \\ &+\frac{3}{16}\left(-\left(\frac{c_{\mathrm{L}}}{c_{\mathrm{T}}}\right)^2+\left(2+\frac{\lambda}{\mu}\right)^2\right)I_5-\frac{3c_{\mathrm{L}}}{8c_{\mathrm{T}}}\left(2+\frac{\lambda}{\mu}\right)I_6+\frac{3c_{\mathrm{L}}^2}{16c_{\mathrm{T}}^2}I_7\Bigg] \end{aligned} \tag{A4}$$

where $I_n := I_n(\xi^2\omega^2/2c_{\mathrm{T}}c_{\mathrm{L}})$,

$$\begin{aligned} f := \frac{\pi\omega^4\mu^2\Delta^2\xi^2}{4\rho D c_{\mathrm{L}}^6}\exp\left[-\frac{\xi^2\omega^2}{4}(c_{\mathrm{T}}^{-2}+c_{\mathrm{L}}^{-2})\right]\Bigg[&-\frac{c_{\mathrm{L}}}{2c_{\mathrm{T}}}\left(2+\frac{\lambda}{\mu}\right)I_0 \\ &+\left(\frac{c_{\mathrm{L}}^2}{2c_{\mathrm{T}}^2}+\frac{1}{4}\left(2+\frac{\lambda}{\mu}\right)^2\right)I_1-\frac{1}{4}\left(\left(\frac{c_{\mathrm{L}}}{c_{\mathrm{T}}}\right)^2+\left(2+\frac{\lambda}{\mu}\right)^2\right)I_3 \\ &+\frac{c_{\mathrm{L}}}{2c_{\mathrm{T}}}\left(2+\frac{\lambda}{\mu}\right)I_4-\frac{1}{4}\left(\frac{c_{\mathrm{L}}}{c_{\mathrm{T}}}\right)^2I_5\Bigg] \end{aligned} \tag{A5}$$

where $I_n := I_n(\xi^2\omega^2/2c_{\mathrm{T}}c_{\mathrm{L}})$,

$$g := \frac{\pi\omega^4\mu^2\Delta^2\xi^2}{4\rho D c_{\mathrm{L}}^6}\exp\left[-\frac{\xi^2\omega^2}{4}(c_{\mathrm{T}}^{-2}+c_{\mathrm{L}}^{-2})\right]$$

$$\times\left[\frac{c_L}{2c_T}\left(2+\frac{\lambda}{\mu}\right)I_0-\frac{1}{4}\left(\left(\frac{c_L}{c_T}\right)^2+\left(2+\frac{\lambda}{\mu}\right)^2\right)I_1\right.$$
$$-\frac{c_L}{2c_T}\left(2+\frac{\lambda}{\mu}\right)I_2+\frac{1}{2}\left(\left(\frac{c_L}{c_T}\right)^2+\left(2+\frac{\lambda}{\mu}\right)^2\right)I_3$$
$$\left.-\frac{c_L}{2c_T}\left(2+\frac{\lambda}{\mu}\right)I_4-\frac{1}{4}\left(2+\frac{\lambda}{\mu}\right)^2I_5+\frac{c_L}{2c_T}\left(2+\frac{\lambda}{\mu}\right)I_6-\frac{c_L^2}{4c_T^2}I_7\right] \tag{A6}$$

where $I_n := I_n(\xi^2\omega^2/2c_Tc_L)$,

$$\tilde{a} := \frac{\pi\omega^4\mu^2\Delta^2\xi^2}{4\rho Dc_T^6}\exp\left[-\frac{\xi^2\omega^2}{4}(c_T^{-2}+c_L^{-2})\right]\left[\frac{c_T}{2c_L}I_0-\frac{1}{4}\left(1+\left(\frac{c_T}{c_L}\right)^2\right)I_1-\frac{c_T}{2c_L}I_2\right.$$
$$\left.+\frac{1}{2}\left(1+\left(\frac{c_T}{c_L}\right)^2\right)I_3-\frac{c_T}{2c_L}I_4-\frac{1}{4}I_5+\frac{c_T}{2c_L}I_6-\frac{c_T^2}{4c_L^2}I_7\right] \tag{A7}$$

where $I_n := I_n(\xi^2\omega^2/2c_Tc_L)$,

$$\tilde{b} := \frac{\pi\omega^4\mu^2\Delta^2\xi^2}{4\rho Dc_T^6}\exp\left[-\frac{\xi^2\omega^2}{4}(c_T^{-2}+c_L^{-2})\right]\left[-\frac{3c_T}{4c_L}I_0+\left(\frac{3}{8}+\left(\frac{3c_T}{4c_L}\right)^2\right)I_1+\frac{3c_T}{8c_L}I_2\right.$$
$$-\frac{9}{16}\left(1+\left(\frac{c_T}{c_L}\right)^2\right)I_3+\frac{3c_T}{4c_L}I_4$$
$$\left.+\frac{3}{16}\left(1-\left(\frac{c_T}{c_L}\right)^2\right)I_5-\frac{3c_T}{8c_L}I_6+\frac{3c_T^2}{16c_L^2}I_7\right] \tag{A8}$$

where $I_n := I_n(\xi^2\omega^2/2c_Tc_L)$,

$$\tilde{c} := \frac{\pi\omega^4\mu^2\Delta^2\xi^2}{4\rho Dc_T^6}\exp\left[-\frac{\xi^2\omega^2}{4}(c_T^{-2}+c_L^{-2})\right]\left[-\frac{c_T}{2c_L}I_0+\left(\frac{1}{4}+\frac{1}{2}\left(\frac{c_T}{c_L}\right)^2\right)I_1\right.$$
$$\left.-\frac{1}{4}\left(1+\left(\frac{c_T}{c_L}\right)^2\right)I_3+\frac{c_T}{2c_L}I_4-\frac{1}{4}\left(\frac{c_T}{c_L}\right)^2I_5\right] \tag{A9}$$

where $I_n := I_n(\xi^2\omega^2 2c_Tc_L)$,

$$\tilde{e} := \frac{3\pi\omega^4\mu^2\Delta^2\xi^2}{4\rho Dc_L^6}\exp\left(-\frac{\xi^2\omega^2}{2c_L^2}\right)\left[-\left(\frac{1}{2}+\frac{3\lambda}{4\mu}+\frac{1}{4}\left(\frac{\lambda}{\mu}\right)^2\right)I_0\right.$$
$$+\left(\frac{13}{16}+\frac{\lambda}{\mu}+\frac{3}{8}\left(\frac{\lambda}{\mu}\right)^2\right)I_1-\left(\frac{1}{4}+\frac{\lambda}{8\mu}\right)I_2$$
$$-\left(\frac{5}{16}+\frac{\lambda}{2\mu}+\frac{5}{16}\left(\frac{\lambda}{\mu}\right)^2\right)I_3+\left(\frac{1}{2}+\frac{3\lambda}{4\mu}+\frac{1}{4}\left(\frac{\lambda}{\mu}\right)^2\right)I_4$$
$$\left.-\left(\frac{7}{16}+\frac{\lambda}{2\mu}+\frac{1}{16}\left(\frac{\lambda}{\mu}\right)^2\right)I_5+\left(\frac{1}{4}+\frac{\lambda}{8\mu}\right)I_6-\frac{1}{16}I_7\right] \tag{A10}$$

where $I_n := I_n(\xi^2\omega^2/2c_L^2)$,

$$\tilde{f} := \frac{\pi\omega^4\mu^2\Delta^2\xi^2}{4\rho Dc_L^6}\exp\left(-\frac{\xi^2\omega^2}{2c_L^2}\right)\left[-\left(3+\frac{7\lambda}{2\mu}+\left(\frac{\lambda}{\mu}\right)^2\right)I_0\right.$$

$$+\left(\frac{11}{2}+\frac{6\lambda}{\mu}+\frac{7}{4}\left(\frac{\lambda}{\mu}\right)^2\right)I_1-\left(4+\frac{4\lambda}{\mu}+\left(\frac{\lambda}{\mu}\right)^2\right)I_2$$
$$+\left(\frac{9}{4}+\frac{2\lambda}{\mu}+\frac{1}{4}\left(\frac{\lambda}{\mu}\right)^2\right)I_3-\left(1+\frac{\lambda}{2\mu}\right)I_4+\frac{1}{4}I_5\Bigg] \tag{A11}$$

where $I_n := I_n(\xi^2\omega^2/2c_L^2)$,

$$\tilde{g} := \frac{\pi\omega^4\mu^2\Delta^2\xi^2}{4\rho D c_L^6}\exp\left(-\frac{\xi^2\omega^2}{2c_L^2}\right)\Bigg[-\left(1+\frac{\lambda}{2\mu}\right)I_0+\left(\frac{9}{4}+\frac{2\lambda}{\mu}+\frac{1}{4}\left(\frac{\lambda}{\mu}\right)^2\right)I_1$$
$$-\left(3+\frac{7\lambda}{2\mu}+\left(\frac{\lambda}{\mu}\right)^2\right)I_2+\left(\frac{7}{2}+\frac{4\lambda}{\mu}+\frac{3}{2}\left(\frac{\lambda}{\mu}\right)^2\right)I_3$$
$$-\left(3+\frac{7\lambda}{2\mu}+\left(\frac{\lambda}{\mu}\right)^2\right)I_4$$
$$+\left(2+\frac{2\lambda}{\mu}+\frac{1}{4}\left(\frac{\lambda}{\mu}\right)^2\right)I_5-\frac{1}{2}\left(2+\frac{\lambda}{\mu}\right)I_6+\frac{1}{4}I_7\Bigg] \tag{A12}$$

where $I_n := I_n(\xi^2\omega^2/2c_L^2)$.

References

[1] Perrin N 1993 *Phys. Rev.* B **48** 12 151
[2] Kanskar M and Wybourne M N 1994 *Phys. Rev.* B **50** 168
[3] Yoh K *et al* 1994 *Semicond. Sci. Technol.* **9** 961
[4] Travis J 1994 *Science* **263** 1702
[5] Ogilvy J A 1987 *Rep. Prog. Phys.* **50** 1553
[6] Luo E Z *et al* 1994 *Phys. Rev.* B **49** 4858
[7] Spanos L and Irene E A 1994 *J. Vac. Sci. Technol.* A **12** 2646
Spanos L *et al* 1994 *J. Vac. Sci. Technol.* A **12(5)** 2653
[8] Maradudin A A and Mills D L 1976 *Ann. Phys., NY* **100** 262
[9] Kirkpatrick T R 1985 *Phys. Rev.* B **31** 5746
[10] Viktorov I A 1970 *Rayleigh and Lamb Waves* (New York: Plenum)
[11] Luttinger J M 1964 *Phys. Rev.* **135** A1505
[12] Flicker J K and Leath P L 1972 *Phys. Rev.* B **7** 2296
[13] Polischuk I Ya *et al* 1988 *Zh. Eksp. Teor. Fiz.* **94** 259 (Engl. Transl. 1988 *Sov. Phys.–JETP* **67** 1881)
[14] Langer J S 1960 *Phys. Rev.* **120** 7145
[15] Eguiluz A G and Maradudin A A 1983 *Phys. Rev.* B **28** 711, 728
[16] McGurn A R and Maradudin A A 1984 *Phys. Rev.* B **30** 3136
[17] Seyler J and Wybourne M N 1990 *J. Phys.: Condens. Matter* **2** 8853
[18] Béal-Monod M T 1993 *Phys. Rev.* B **47** 3495
[19] Thouless D J 1977 *Phys. Rev. Lett.* **39** 1167
[20] Jäckle J 1981 *Solid State Commun.* **39** 1261
[21] Böttger H and Damker Th 1994 *Phys. Rev.* B **50** 12509